



0040-4020(95)01080-7

Conformational Analysis of a Marine Antineoplastic Macrolide, Bryostatin 10¹⁾

Yoshiaki Kamano* and Hui-ping Zhang

Faculty of Science, Kanagawa University, Hiratsuka 259-12, Japan

Hiroshi Morita and Hideji Itokawa

Department of Pharmacognosy, School of Pharmacy, Tokyo University of Pharmacy & Life Science, 1432-1 Horinouchi, Hachioji, Tokyo 192-03, Japan

Osamu Shiota

Division of Pharmacognosy and Phytochemistry, National Institute of Health Sciences, 1-18-1 Kamiyoga, Setagaya-ku, Tokyo 158, Japan

George R. Pettit, Delbert L. Herald and Cherry L. Herald

Department of Chemistry, Arizona State University, Tempe, Arizona 85287-1604, USA

Abstract: Conformation of bryostatin 10, a marine antineoplastic macrolide, in CDCl₃ was analyzed by the spectroscopic and computational chemical methods. A combination of homonuclear two-dimensional NMR techniques at 600 MHz have enabled us to perform complete assignment of the ¹H signals of bryostatin 10 in CDCl₃. The conformation of its solution form was elucidated by a phase sensitive ROESY spectrum, temperature effect on OH proton and ³J vicinal coupling constants. Restrained molecular-dynamics simulation led to a well defined conformation of the compound in solution, which was found to be homologous to that of bryostatin 2 observed in the solid state.

Habitat of a marine bryozoan *Bugula neritina* (Linnaeus) is distributed widely over the Atlantic, Pacific and Arabic oceans. This abundant sea-mat is well known as a ship fouling species. However, *B. neritina* has been found to be a precious source of antineoplastic polyether macrolides, bryostatins 1 - 15.²⁾ Bryostatin 1,³⁾ the first member of this series is currently under clinical trials as an anticancer agent. Bryostatins have attracted research interest not only as promising drug candidates but also as unique biochemical probes.

The structures of bryostatins have been elucidated by a combination of extensive 2D NMR studies, and the structures of bryostatins 1³⁾ and 24⁴⁾ have further been confirmed by the X-ray crystallographic studies. It is well known that biological properties of bioactive macrocyclic polyethers, cyclic peptides and the like are critically dependent on their conformations.⁵⁾ In order to

probe the backbone conformational requirements to show antineoplastic activity, the conformations of antitumor bryostatins must be first elucidated. However, no conformational analysis of bryostatin molecules in solution has been published.

Here, we made conformational analysis of bryostatin 10 in CDCl₃ and compared the results with the conformation of bryostatin 2, another antitumor bryostatin whose absolute structure has been determined by X-ray analysis.

By high field NMR studies at 600 MHz in CDCl₃ including studies on ROE, temperature effect on OH protons and ³J vicinal coupling constants, and restrained molecular dynamics *in vacuo*, complete assignment and coupling network of the ¹H signals of the molecule, and accordingly analysis of its conformational dynamics in solution were made. The preferred ring conformation of bryostatin 10 was predicted by a high temperature molecular dynamics calculation method, employing distance restraint. The ³J proton NMR coupling constants were calculated from the dynamics simulation of the isolated bryostatin 10 and compared with the experimental data. This gave a possible reinterpretation of the experimental data.

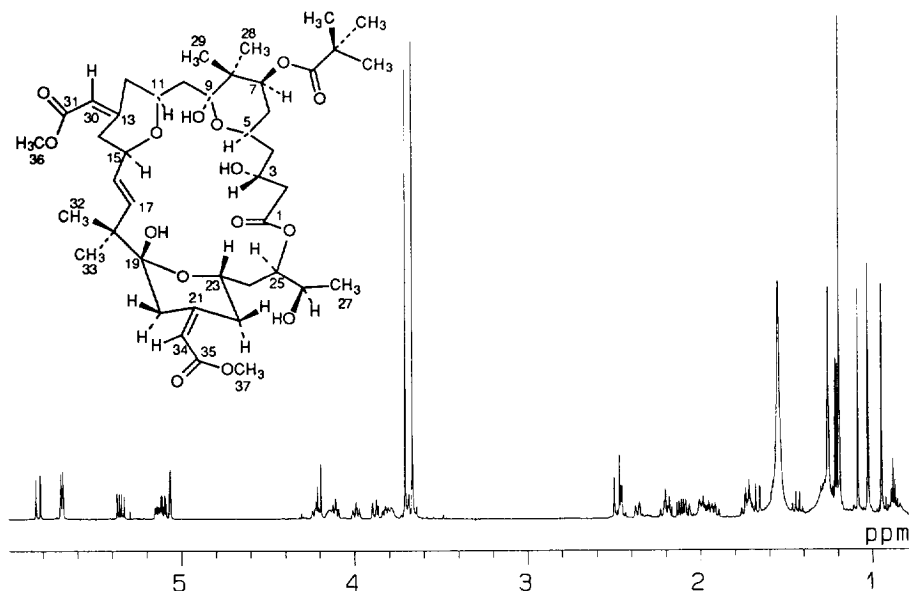


Fig. 1. A structure of bryostatin 10 and its ¹H NMR spectrum in CDCl₃ at 600 MHz.

Complete assignments of ¹H NMR signals and coupling constants in CDCl₃

The first step of the studies for elucidation of the solution conformation of bryostatin 10, is the complete assignments of ¹H signals in various NMR measurements. The NMR data of bryostatin 10 in CDCl₃ have already been reported. However, most of the ¹H signals in the region around 2 and 4 ppm, where a number of signals are observed, have been reported simply as multiplets.⁶⁾ At 600

MHz, such signals in the crowded region gave good resolution. Only one set of peaks observed in the ^1H NMR spectrum indicates that bryostatin 10 predominantly exists in one conformation in solution. The ^1H spin systems were identified by DQF-COSY and HOHAHA spectra. The ^3J homonuclear coupling constants were obtained from one-dimensional ^1H NMR spectrum. All the proton chemical shifts and coupling constants are listed in Table 1. The rigidity of the bryostatin backbone is suggested by the magnetic non-equivalence of the geminal methylene protons at C-2, C-4, C-6, C-10, and so on in Table 1.

Table 1. Chemical shifts (δ ppm) of ^1H NMR signals of bryostatin 10 and their ROE relationships

Position	^1H (J/Hz) ^a	ROEs ^b (Counter part protons and ROE strength)
2 α	2.46 dd (12.1, 15.0)	3 (m), 3-OH (s), 4 β (w), 5 (s)
2 β	2.48 d (15.0)	5 (w), 11(m)
3	4.15 m	4 β (w), 4 α (w), 23 (w), 19-OH (m)
3-OH	4.21 d (12.1)	19-OH (m)
4 β	1.57 dd (11.7, 12.5)	4 α (s), 5 (m)
4 α	1.99 ddd (12.5, 2.9, 2.1)	5 (w), 3-OH (w), 6 β (w)
5	4.22 tdd (11.7, 2.2, 2.6)	6 α (w), 7 (m)
6 β	1.43 q (12.0)	6 α (s), 29 (m), 7 (w)
6 α	1.73 tdd (11.7, 4.8, 2.6)	7 (m)
7	5.11 dd (11.7, 4.8)	28 (m)
9-OH	2.51 br s	11 (m)
10 α	1.67 d (15.0)	10 β (s), 11(w), 12 β (w), 28 α (m)
10 β	2.12 dd (15.0, 7.7)	29 β (m)
11	3.82 ddd (11.4, 7.7, 2.6)	12 α (w), 12 β (w), 15 (m)
12 α	2.07 dt (13.6, 2.6)	12 β (s), 30 (m)
12 β	2.21 (br t, 12.1)	
14 β	1.91 br t (12.0)	14 α (s), 15 (m)
14 α	3.68 br d (12.0)	
15	4.11 ddd (11.0, 8.4, 2.6)	16 (m), 17 (m)
16	5.35 dd (15.8, 8.4)	17 (m), 32 β (m)
17	5.83 d (15.8)	19-OH (m), 25 (w), 33 α (w)
19-OH	5.07 d (2.9)	32 β (w), 3' (w)
20 β	2.19 br d (13.2)	20 α (s), 32 β (m), 34 (m)
20 α	2.36 br dd (13.2, 2.2)	19-OH (w), 22 α (w), 33 α (m)
22 α	1.74 br t (13.5)	22 β (s), 23 (m)
22 β	3.88 br t (12.8)	24 β (m)
23	3.98 tt (11.4, 2.6)	24 β (m)
24 α	1.72 ddd (14.7, 11.4, 3.0)	24 β (s), 25 (m)
24 β	1.95 ddd (14.7, 12.1, 2.9)	25 (m), 26 (w)
25	5.14 ddd (12.1, 5.7, 3.0)	26 (w)
26	3.79 m	27 (m)
26-OH	not observed	
27	1.21 d (6.2)	
28 α	0.95 s	29 (m), 3' (w)
29 β	1.03 s	
30	5.69 t (2.6)	
32 β	1.03 s	
33 α	1.09 s	
34	5.70 s	
36	3.71 s	
37	3.67 s	
3'	1.19 s	
4'	1.19 s	
5'	1.19 s	

^a The signals were recorded at 600 MHz in CDCl_3 .

^b The s, m and w letters in the parenthesis indicate strong, medium and weak ROE enhancements.

ROE relationship of bryostatin 10

A phase sensitive ROESY spectrum⁷⁾ at 600 MHz gave information about the solution conformation of bryostatin 10. The intense of all the ROE correlations were clarified into three ranges; strong, medium and weak (Table 1). Stereospecific assignments of each methylene proton on the basis of their coupling constants, were confirmed by the ROE studies. Apart from sequential correlations, there are three ROEs that are of particular importance with regard to its backbone conformation. They are the medium ROE enhancements between the hydroxy proton at C-3 and the hydroxy proton at C-19, and between the proton at C-3 and the hydroxy proton at C-19, indicating that they are very close to each other and/or forming an intramolecular hydrogen bond between the two hydroxyl groups, and another ROE enhancement between H-25 and one of the olefinic protons (H-17). These ROEs across the 26-membered macrolide ring system suggest restriction of the conformation of the ring and that the backbone ring system is taking a roughly scoop-shaped molecular structure. The other hydroxy protons at C-9 and C-26 did not show any ROE correlations.

The conformations of the three tetrahydropyran rings were concluded to be all of chair form, as in the crystal form of bryostatins 1 and 2, on the basis of the ROE correlations between 1, 3-diaxial protons; H-5 - H-7, H-11 - H-15, and H-20 α - H-22 α . In addition to the above enhancements, a strong ROE enhancement was observed between H-2 α and H-5, suggesting that the conformation of the carbon chain from C-1 to C-5 did not take a zigzag form.

Hydrogen bonds in bryostatin 10

The presence of intramolecular hydrogen bonds was suggested by the IR absorption band at 3474 cm^{-1} in a highly dilute solution of bryostatin 10 in CCl_4 (0.0037 M) and the doublet signals of OH protons both at C-3 and C-19 in the ^1H NMR spectrum.

^1H NMR assay of peptidic compounds is known to provide information about intramolecular hydrogen bonds and accordingly about conformation of macrocyclic peptidic compounds in solution: low temperature dependence of amide hydrogens means that it is either involved in hydrogen bonds or shielded by solvent.⁸⁾ In the ^1H NMR spectrum of bryostatin 10 in CDCl_3 , the following temperature dependence of OH proton resonances were observed (Table 2): the OH protons at C-3 and C-19 showed small temperature coefficients and the OH proton at C-9 was slightly shifted in a higher field. The OH proton signal at C-26 was not observed in this experiment. No report has referred to the applicability of the empirically established rule of amide protons to OH protons yet, if we apply this rule of amide protons to hydroxy protons, the data of Table 2 further suggest that in solution conformation, bryostatin 10 contains hydrogen bondings involving C-3 and C-19 OH protons as in the solid state conformation of bryostatin 2, which was established by crystallography. Further studies are being made on the relation of the temperature coefficient and the nature of hydro-

Table 2 Temperature coefficients ($-\text{d}\delta/\text{d}T \times 10^3$ ppm/K) of chemical shifts of OH signals of bryostatin 10 in CDCl_3 measured at ten intervals over the range 300 - 320 K.

	3-OH	9-OH	19-OH	26-OH
coefficients	0.8	6.4	1.6	not detected

gen bonds.

Restrained MD calculation of bryostatin 10

To study conformational dynamics of bryostatin 10 in solution, MD calculation was performed by using MM2* force field in MacroModel / Batchmin⁹⁾ (Ver. 4.5). The dielectric constant (ϵ) is considered to be proportional to interatomic distances (r). The MD calculations were performed in a thermal bath at 900 K by using a time step of 1.0 fs and equilibrated for a duration of 100 ps. This temperature was chosen after several trial- and error tests, judging from the arrival at equilibrium between possible conformers. Solvent molecules were not included in the calculations. The starting structure of bryostatin 10 was modeled from the X-ray geometry of bryostatin 2.⁴⁾ The preliminary insights using ROE relationship (Table 1) into the conformation were used to understand the conformational properties of bryostatin 10. The distance constraints derived from the volume of the cross peaks in ROESY spectrum were classified into three ranges, 1.8 - 2.5 Å, 1.8 - 3.5 Å and 1.8 - 5.0 Å, corresponding to strong, medium and weak ROEs, respectively, as shown in Table 1. In addition, the factor of +1.5Å was added to methyl groups. A total of 49 distance restraints derived from a phase sensitive ROESY spectrum were applied to a skewed biharmonic constraining function in the MD simulations. No hydrogen bonding and dihedral angle restraints were taken into consideration. The 1000 sampled conformers generated by MD calculation were finally minimized by the use of molecular mechanics calculation of MM2* force field. All heavy atoms (carbons and oxygens) comparison was performed to eliminate duplicate conformations and the maximum allowed atomic deviation for identical conformation was set to 0.25 Å. In the MD calculation, the lowest energy conformation was found 7 times and 20 conformers at 85 times were found within 1 kcal/mol of the global minimum energy (RMSD=0.701Å for the best fit of heavy atoms). The global minimum structure is shown in Fig. 2. The total energy of the lowest energy conformer was 304.5 kJ/mol. In addition, the conformer completely satisfied the distance constraints derived from the

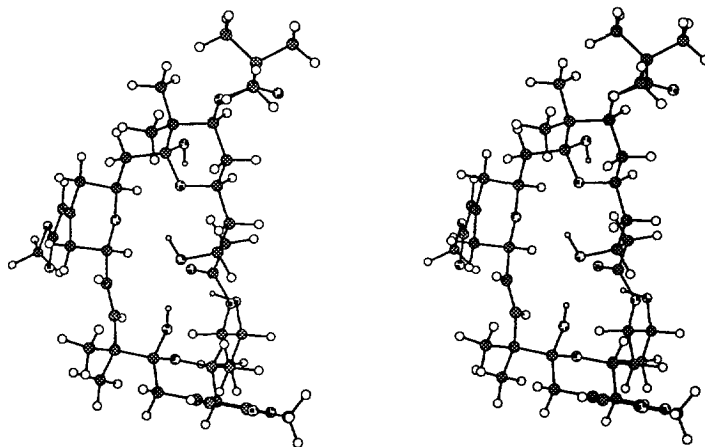


Fig.2 Stereoscopic view of the lowest energy conformer of bryostatin 10 obtained by the MD and MM calculations

characteristic ROE relationship. This result was also supported by the comparison with the solution structure of bryostatin 10 as obtained from NMR data.

The root-mean-square (r.m.s.) difference between the atoms in the starting structure derived from the X-ray structure of bryostatin 2 and the corresponding atoms of the calculated structure *in vacuo* was 1.109 Å (Fig. 3). Hence, the final structure obtained from the *in vacuo* calculations is independent from the starting conformation.

The torsion angles in the global minimum structure are given in Table 3. Only two torsions in the ring system showed significant differences between bryostatin 10 and bryostatin 2. The differences at C-15 - C-16 and C-17 - C-18 torsions around the trans olefinic bond were 21.7° and 19.2°, respectively. These differences agree with the fact that the spin-lattice relaxation times (T1) (C-16: 300, C-17: 361 msec), reported in our previous paper,^{6b)} were larger than

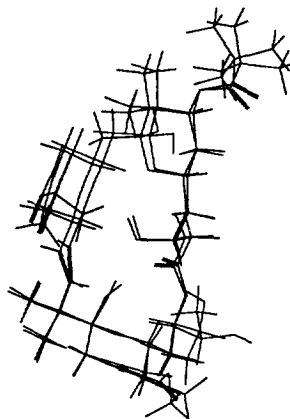


Fig.3 Superimposed structures of the starting structure of bryostatin 10 and that obtained by energy minimizations (RMSD=1.109Å).

Table 3. Backbone torsion angles of bryostatin 10 calculated from the global minimum structure and those of bryostatin 2 from the X-ray structure.⁴⁾

torsion	bryostatin 10	bryostatin 2
O1-1-2-3	-61.4	-60.9
1-2-3-4	179.9	175.9
2-3-4-5	48.2	48.5
3-4-5-6	173.4	177.3
4-5-6-7	-177.0	-172.9
5-6-7-8	55.2	58.3
6-7-8-9	-53.0	-58.5
7-8-9-10	177.3	175.7
8-9-10-11	-173.9	175.8
9-10-11-12	-158.7	-141.4
10-11-12-13	-175.6	-178.3
11-12-13-14	56.1	54.8
12-13-14-15	-55.7	-53.8
13-14-15-16	177.6	169.4
14-15-16-17	88.2	109.9
15-16-17-18	-179.3	-179.7
16-17-18-19	-97.7	-116.9
17-18-19-20	179.6	176.4
18-19-20-21	173.8	175.0
19-20-21-22	-55.8	-51.5
20-21-22-23	58.4	51.3
21-22-23-24	-176.5	-170.9
22-23-24-25	173.3	179.1
23-24-25-O1	54.2	51.9

The values are given in degrees.

those of the other olefinic carbons (C-30 and C-34). In addition, the T1 value (1162 msec) of the methoxy methyl group of C-36 was larger than those of the other methyl groups. This may also be related to the large motion of the C-30 - C-31 torsion angles in the MD calculation.

In the global minimum structure, the interatomic distances between the hydrogens of 19-OH and 3-OH, between the hydrogen of 19-OH and H-3, and between H-17 and H-25 were 2.68, 1.93, and 2.92 Å, respectively, which satisfied the ROE relationship mentioned above. The hydrogen bonding between 19-OH and the oxygen of 3-OH is present during 73.5 % of the MD simulation. It is consistent with the low temperature coefficient of the 19-OH proton. In addition, the hydrogen bonds between 3-OH and O5, and between 3-OH and O11 are observed during 58.9 and 43.5 %, respectively. They are

also consistent with the low temperature coefficient of the 3-OH proton. In Table 4, interatomic distances between the oxygens and bond angles of the hydrogens involved in intramolecular hydrogen bonds in the global minimum structure are summarized. The hydrogen of 19-OH was strongly hydrogen bonded to the hydroxy oxygen at C-3, and the hydrogen of 3-OH was strongly hydrogen bonded to the two oxygen atoms in the tetrahydropyran rings.

Table 4 Interatomic distances between oxygens and bond angles of hydrogen involved in hydrogen bonds of the global minimum structure of bryostatin 10, and of the X-ray structures of bryostatins 1³) and 2.⁴)

Two oxygen atoms		bryostatin 10		bryostatin 1	bryostatin 2
		distance (Å)	OH...O angle (°)	distance (Å)	distance (Å)
19-OH	3-OH	2.81	154.2	2.71	2.72
3-OH	O5	2.81	135.5	2.84	2.78
3-OH	O11	2.98	137.0	3.00	3.05

The obtained minimum energy conformation of bryostatin 10 delivered by MM2* force field was essentially identical to the original conformation deduced on the basis of NMR data in solution.

Prediction of ³J proton coupling constants

Table 5. Observed and calculated ³J proton coupling constants^a) of the global minimum structure of bryostatin 10 obtained by MD calculation.

position	observed	calculated
2β/3	not detected	1.8
2α/3	12.1	11.4
3/4b	0.0	3.0
3/4a	2.9	3.4
4b/5	11.7	11.6
4a/5	2.2	2.9
5/6b	11.7	11.7
5/6a	2.6	2.6
6b/7	11.7	11.2
6a/7	4.8	4.6
10b/11	7.7	9.9
10a/11	0.0	1.0
11/12b	11.4	11.6
11/12a	2.6	2.2
14b/15	11.0	11.6
14a/15	2.6	2.0
22b/23	2.6	2.0
22a/23	11.4	11.6
23/24b	2.9	2.7
23/24a	11.4	11.7
24b/25	12.1	11.7
24a/25	3.0	2.5

^a calculated by using an electronegativity sensitive Karplus equation¹⁰⁾

Three-bond couplings gave very useful information for the determination of the backbone conformation because they can directly be converted into dihedral angles via the Karplus-type equation. The ³J proton coupling constants (Table 1) were calculated from the global minimum structure generated by MD simulation *in vacuo*, by using an electronegativity sensitive Karplus equation.¹⁰⁾ These have been compared with the experimental coupling constants. As can be seen from Table 5, the observed coupling constants are similar to those calculated from the global minimum conformer of bryostatin 10, indicating that conformation of bryostatin 10 is homologous to that observed in the solid state of bryostatin 2.

Conclusion

High field NMR, and a ROE-constrained MD and energy minimization-conformational search narrowly defined the backbone conformation of bryostatin 10. In spite of a relatively large membered ring in the backbone, the results converged to a conformation of bryostatin 10 in CDCl₃ which was

found to be homologous to the X-ray structure of bryostatin 2. We are also interested in the solution conformation of bryostatin 10 in biological system and the relationship between the solution conformers and its biological activities. Further investigation is currently in progress.

Experimental

Isolation

Bryostatin 10 was isolated from the CH₂Cl₂ extract of the *Bugula neritina*, which was collected off the Gulf of Aomori (1.5 kg, wet weight), Asamushi, Aomoriken (Japan), by a series of chromatographies such as Sephadex LH-20 and reversed phase HPLC.¹¹⁾

NMR

All experiments were carried out on a JEOL α 600 spectrometer. For all 2D experiments, the concentration was 3 mg/ml in CDCl₃. The spectra were recorded at 300K. The temperature gradients of the hydroxyl protons were recorded in the range of 300 - 320 K for CDCl₃. A phase sensitive ROESY experiment was acquired with mixing times of 250 msec to predict the H-H distances of bryostatin 10 in solution.

Computational Methods

Computer modeling was carried out with the MACROMODEL program (version 4.5) on a IRIS 4D computer (Indy R4600 and Power CHALLENGE R8000). Molecular mechanics and dynamics calculations were performed with the MM2* force field with a distance-dependent dielectric, $\epsilon=R_{ij}$. The simulations were run at 900 K with 1.0-fs time steps for an equilibration period of 20 ps. The simulation was continued for 100 ps. Structures were sampled by time at 0.1-ps intervals. Extended cutoff distances were employed (8 Å in van der Waals, 20 Å in charge/electrostatics and 10 Å in charge/multipole electrostatics). Constrained dynamics were calculated with an extra harmonic term of the form $k(\theta-\theta_0)$ added to the force field ($k=100$). Structures from the dynamics trajectories were energy minimized with the derivative convergence criteria at a value of 0.001 kJ/Å-mol.

References and Notes

- 1) 37th SYMPOSIUM ON THE CHEMISTRY OF NATURAL PRODUCTS, TOKUSHIMA, SYMPOSIUM PAPERS pp 672-677.
- 2) a) G. R. Pettit, in: "Progress in the Chemistry of Organic Natural Products." Ed. by W. Herz, G. W. Kirby, W. Steglich and Ch. Tamm, Springer-Verlag, New York, 1991, Vol. 57, pp. 153-195; b) G. R. Pettit, F. Gao, D. Sengupta, J. C. Coll, C. L. Herald, D. L. Doubek, J. M. Schmidt, J. R. Van Camp, J. J. Rudloe, and R. A. Nieman, *Tetrahedron*, **1991**, 47, 3601.
- 3) G. R. Pettit, C. L. Herald, D. L. Doubek, and D. L. Herald, *J. Am. Chem. Soc.*, **1982**, 104, 6846.
- 4) a) G. R. Pettit, D. L. Herald, F. Gao, D. Sengupta, and C. L. Herald, *J. Org. Chem.*, **1991**, 56, 1337; b) Structure of bryostatin 2 was showed in Fig. 4.
- 5) V. J. Hruby and M. E. Hadley, in: "Design and Synthesis of Organic Molecules Based on Molecular Recognition." Ed. by G. Van Binst, Springer-Verlag, Heidelberg, 1986, pp. 269-286.
- 6) a) G. R. Pettit, Y. Kamano, and C. L. Herald, *J. Org. Chem.*, **1987**, 52, 2848; b) Y. Kamano, H.-p. Zhang, A. Hino, M. Yoshida, G. R. Pettit, C. L. Herald, and H. Itokawa, *J. Nat. Prod.*, in press.
- 7) A. A. Bothner-By, R. L. Stephens, J. Lee, C. D. Warren and R. W. Jeanloz, *J. Am. Chem. Soc.*, **1984**, 106, 811.
- 8) H. Kessler, *Angew. Chem.*, **1982**, 94, 509; *ibid.*, int. Ed., **1982**, 21, 512.
- 9) F. Mohamadi, N. G. J. Richards, W. C. Guida, R. Liskamp, M. Lipton, C. Caufield, G. Chang, T. Hendrickson and W. C. Still, *J. Comput. Chem.*, **1990**, 11, 440.
- 10) C. A. G. Haasnoot, F. A. A. M. De Leeuw, C. Altona, *Tetrahedron*, **1980**, 36, 2783.
- 11) General methods and isolation are the same as those described in the previous report.^{6b)}

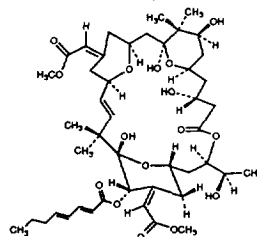


Fig.4 A structure of bryostatin 2